

## Acid–Base Actuation of [c2]Daisy Chains

Lei Fang,<sup>†</sup> Mohamad Hmadeh,<sup>‡</sup> Jishan Wu,<sup>§,||</sup> Mark A. Olson,<sup>†</sup> Jason M. Spruell,<sup>†</sup> Ali Trabolssi,<sup>†</sup> Ying-Wei Yang,<sup>§,⊥</sup> Mourad Elhabiri,<sup>‡</sup> Anne-Marie Albrecht-Gary,<sup>\*,‡</sup> and J. Fraser Stoddart<sup>\*,†</sup>

*Department of Chemistry, Northwestern University, 2145 Sheridan Road, Evanston, Illinois 60208-3113, Laboratoire de Physico-Chimie Bioinorganique, UDS-CNRS (UMR 7177), Institut de Chimie de Strasbourg, Université de Strasbourg, ECPM, 25 Rue Becquerel, 67200 Strasbourg, France, and Department of Chemistry and Biochemistry, University of California, Los Angeles, 405 Hilgard Avenue, Los Angeles, California 90095-1569*

Received February 3, 2009; E-mail: stoddart@northwestern.edu; amalbre@chimie.u-strasbg.fr

**Abstract:** A versatile synthetic strategy, which was conceived and employed to prepare doubly threaded, bistable [c2]daisy chain compounds, is described. Propargyl and 1-pentenyl groups have been grafted onto the stoppers of [c2]daisy chain molecules obtained using a template-directed synthetic protocol. Such [c2]daisy chain molecules undergo reversible extension and contraction upon treatment with acid and base, respectively. The dialkyne-functionalized [c2]daisy chain (AA) was subjected to an [AA+BB] type polymerization with an appropriate diazide (BB) to afford a linear, mechanically interlocked, main-chain polymer. The macromolecular properties of this polymer were characterized by chronocoulometry, size exclusion chromatography, and static light-scattering analysis. The acid–base switching properties of both the monomers and the polymer have been studied in solution, using <sup>1</sup>H NMR spectroscopy, UV/vis absorption spectroscopy, and cyclic voltammetry. The experimental results demonstrate that the functionalized [c2]daisy chains, along with their polymeric derivatives, undergo quantitative, efficient, and fully reversible switching processes in solution. Kinetics measurements demonstrate that the acid/base-promoted extension/contraction movements of the polymeric [c2]daisy chain are actually faster than those of its monomeric counterpart. These observations open the door to correlated molecular motions and to changes in material properties.

### Introduction

The mechanical bond<sup>1</sup> is the distinguishing characteristic of mechanically interlocked molecules (MIMs) such as catenanes and rotaxanes.<sup>2</sup> MIMs are true molecular entities as a result of their mechanically interlocked components being intrinsically linked to one another — resulting in a mechanical bond which prevents dissociation of the components unless one or more covalent bonds are cleaved. The dynamic nature of mechanical

bonds allows for the components to undergo relative internal movements, i.e., translation and circumrotation, within the MIMs. Many examples of nanomachines/nanoswitches<sup>3</sup> operating at the molecular level, such as molecular actuators,<sup>4</sup> molecular electronic components,<sup>5</sup> molecular nanovalves,<sup>6</sup> etc., have been developed, based on either bistable catenanes<sup>7</sup> or bistable rotaxanes<sup>8</sup> as the MIMs.

Artificial molecular actuators, which can convert chemical,<sup>9</sup> electrochemical,<sup>10</sup> or photochemical<sup>11</sup> energy into mechanical

<sup>†</sup> Northwestern University.

<sup>‡</sup> Université de Strasbourg.

<sup>§</sup> University of California, Los Angeles.

<sup>||</sup> Present Address: Department of Chemistry, National University of Singapore, 3 Science Drive 3, Singapore 117543.

<sup>⊥</sup> Present Address: Department of Chemistry, 1102 Natural Sciences 2, University of California, Irvine, California 92697-2025 (USA).

(1) (a) Jager, R.; Vögtle, F. *Angew. Chem., Int. Ed.* **1997**, *36*, 930–944. (b) Stoddart, J. F.; Colquhoun, H. M. *Tetrahedron* **2008**, *64*, 8231–8263.

(2) (a) Amabilino, D. B.; Stoddart, J. F. *Chem. Rev.* **1995**, *95*, 2725–2828. (b) Breault, G. A.; Hunter, C. A.; Mayers, P. C. *Tetrahedron* **1999**, *55*, 5265–5293. (c) Hubin, T. J.; Busch, D. H. *Coord. Chem. Rev.* **2000**, *200*, 5–52. (d) Schalley, C. A.; Weilandt, T.; Bruggemann, J.; Vögtle, F. *Top. Curr. Chem.* **2004**, *248*, 141–200. (e) Vickers, M. S.; Beer, P. D. *Chem. Soc. Rev.* **2007**, *36*, 211–225.

(3) (a) Balzani, V.; Credi, A.; Raymo, F. M.; Stoddart, J. F. *Angew. Chem., Int. Ed.* **2000**, *39*, 3349–3391. (b) Ballardini, R.; Balzani, V.; Credi, A.; Gandolfi, M. T.; Venturi, M. *Acc. Chem. Res.* **2001**, *34*, 445–455. (c) Kay, E. R.; Leigh, D. A.; Zerbetto, F. *Angew. Chem., Int. Ed.* **2007**, *46*, 72–191. (d) Balzani, V.; Credi, A.; Venturi, M. *ChemPhysChem* **2008**, *9*, 202–220.

(4) (a) Collin, J. P.; Dietrich-Buchecker, C.; Gavina, P.; Jimenez-Molero, M.-C.; Sauvage, J.-P. *Acc. Chem. Res.* **2001**, *34*, 477–487. (b) Hanke, A.; Metzler, R. *Chem. Phys. Lett.* **2002**, *359*, 22–26. (c) Liu, Y.; Flood, A. H.; Bonvallet, P. A.; Vignon, S. A.; Northrop, B. H.; Tseng, H.-R.; Jeppesen, J. O.; Huang, T. J.; Brough, B.; Baller, M.; Magonov, S.; Solares, S. D.; Goddard, W. A.; Ho, C.-M.; Stoddart, J. F. *J. Am. Chem. Soc.* **2005**, *127*, 9745–9759. (d) Bonnet, S.; Collin, J. P.; Koizumi, M.; Mobian, P.; Sauvage, J.-P. *Adv. Mater.* **2006**, *18*, 1239–1250. (e) Juluri, B. K.; Kumar, A. S.; Liu, Y.; Ye, T.; Yang, Y.-W.; Flood, A. H.; Fang, L.; Stoddart, J. F.; Weiss, P. S.; Huang, T. J. *ACS Nano* **2009**, *3*, 291–300.

(5) (a) Collier, C. P.; Wong, E. W.; Belohradsky, M.; Raymo, F. M.; Stoddart, J. F.; Kuekes, P. J.; Williams, R. S.; Heath, J. R. *Science* **1999**, *285*, 391–394. (b) Flood, A. H.; Stoddart, J. F.; Steuerman, D. W.; Heath, J. R. *Science* **2004**, *306*, 2055–2056. (c) Norgaard, K.; Laursen, B. W.; Nygaard, S.; Kjaer, K.; Tseng, H.-R.; Flood, A. H.; Stoddart, J. F.; Bjornholm, T. *Angew. Chem., Int. Ed.* **2005**, *44*, 7035–7039. (d) Green, J. E.; Choi, J. W.; Boukai, A.; Bunimovich, Y.; Johnston-Halperin, E.; DeIonno, E.; Luo, Y.; Sheriff, B. A.; Xu, K.; Shin, Y. S.; Tseng, H.-R.; Stoddart, J. F.; Heath, J. R. *Nature (London)* **2007**, *445*, 414–417.

motion, have the potential for spawning nanoelectromechanical systems (NEMS).<sup>4,9–11</sup> Current investigations have focused on the development of the “bottom-up” approach,<sup>12</sup> which is centered on the design and manipulation of macromolecules and molecular assemblies, both biological and artificial, with the aim of transferring<sup>13</sup> molecular phenomena into nano/microscale motions. To achieve macroscopic-material property changes from the molecular arena, much effort has been devoted to the design and synthesis of mechanically interlocked macromol-

ecules, such as polymeric,<sup>14</sup> oligomeric,<sup>15</sup> or dendritic<sup>16</sup> rotaxanes and catenanes. The incorporation of bistability into these macromolecules, resulting in mechanically interlocked switchable polymeric scaffolds (MISPS),<sup>17</sup> is a valuable example of the “bottom-up” approach taken by chemists to transform motions at the molecular level into changes in properties in the nano-, micro-, and macroscale regimes. However, to date, formidable challenges still remain in the production of MISPS on account of their structural complexity and sensitivity to many reaction conditions, in addition to the inefficient, multistep synthetic sequences required for their preparation.

Acid–base switchable bistable systems have been studied<sup>18</sup> extensively over the past decade. Typically a crown ether, e.g., dibenzo[24]crown-8 ring (DB24C8), is employed as the encircling macrocycle, while a dialkylammonium center ( $-\text{CH}_2-\text{NH}_2^+\text{CH}_2-$ ) and an *N,N'*-dialkylated-4,4'-bipyridinium unit (BYPM<sup>2+</sup>) are used as the recognition sites for the macrocycle. Since the association constants for the 1:1 complex formed between DB24C8 and ( $-\text{CH}_2\text{NH}_2^+\text{CH}_2-$ )<sup>18a</sup>/BYPM<sup>2+</sup><sup>18d</sup> in MeCN are 420/82 M<sup>-1</sup> respectively, it is hardly surprising that the DB24C8 ring encircles the dialkylammonium center predominantly. Upon deprotonation, however, of the ( $-\text{CH}_2-\text{NH}_2^+\text{CH}_2-$ ) center, the DB24C8 ring moves from this site to the BYPM<sup>2+</sup> unit, on account of the drastically reduced binding affinity between the DB24C8 and the resulting neutral

- (6) (a) Nguyen, T. D.; Tseng, H.-R.; Celestre, P. C.; Flood, A. H.; Liu, Y.; Stoddart, J. F.; Zink, J. I. *Proc. Natl. Acad. Sci. U.S.A.* **2005**, *102*, 10029–10034. (b) Patel, K.; Angelos, S.; Dichtel, W. R.; Coskun, A.; Yang, Y.-W.; Zink, J. I.; Stoddart, J. F. *J. Am. Chem. Soc.* **2008**, *130*, 2382–2383. (c) Angelos, S.; Yang, Y.-W.; Patel, K.; Stoddart, J. F.; Zink, J. I. *Angew. Chem., Int. Ed.* **2008**, *47*, 2222–2226.
- (7) (a) Asakawa, M.; Ashton, P. R.; Balzani, V.; Credi, A.; Hamers, C.; Matternsteig, G.; Montalti, M.; Shipway, A. N.; Spencer, N.; Stoddart, J. F.; Tolley, M. S.; Venturi, M.; White, A. J. P.; Williams, D. J. *Angew. Chem., Int. Ed.* **1998**, *37*, 333–337. (b) Collier, C. P.; Matternsteig, G.; Wong, E. W.; Luo, Y.; Beverly, K.; Sampaio, J.; Raymo, F. M.; Stoddart, J. F.; Heath, J. R. *Science* **2000**, *289*, 1172–1175. (c) Ikeda, T.; Saha, S.; Aprahamian, I.; Leung, K. C.-F.; Williams, A.; Deng, W.-Q.; Flood, A. H.; Goddard, W. A., III; Stoddart, J. F. *Chem. Asian J.* **2007**, *2*, 76–93.
- (8) (a) Bissell, R. A.; Cordova, E.; Kaifer, A. E.; Stoddart, J. F. *Nature (London)* **1994**, *369*, 133–137. (b) Jeppesen, J. O.; Perkins, J.; Becher, J.; Stoddart, J. F. *Angew. Chem., Int. Ed.* **2001**, *40*, 1216–1221. (c) Tseng, H.-R.; Vignon, S. A.; Celestre, P. C.; Perkins, J.; Jeppesen, J. O.; Di Fabio, A.; Ballardini, R.; Gandolfi, M. T.; Venturi, M.; Balzani, V.; Stoddart, J. F. *Chem.–Eur. J.* **2004**, *10*, 155–172. (d) Zhao, Y.-L.; Dichtel, W. R.; Trabolsi, A.; Saha, S.; Aprahamian, I.; Stoddart, J. F. *J. Am. Chem. Soc.* **2008**, *130*, 11294–11296.
- (9) (a) Tseng, H.-R.; Vignon, S. A.; Stoddart, J. F. *Angew. Chem., Int. Ed.* **2003**, *42*, 1491–1495. (b) Huang, T. J.; Brough, B.; Ho, C.-M.; Liu, Y.; Flood, A. H.; Bonvallet, P. A.; Tseng, H.-R.; Stoddart, J. F.; Baller, M.; Magonov, S. *Appl. Phys. Lett.* **2004**, *85*, 5391–5393. (c) Huang, T. J.; Flood, A. H.; Brough, B.; Liu, Y.; Bonvallet, P. A.; Kang, S. S.; Chu, C. W.; Guo, T. F.; Lu, W. X.; Yang, Y.; Stoddart, J. F.; Ho, C.-M. *IEEE T. Autom. Sci. Eng.* **2006**, *3*, 254–259.
- (10) (a) Bermudez, V.; Capron, N.; Gase, T.; Gatti, F. G.; Kajzar, F.; Leigh, D. A.; Zerbetto, F.; Zhang, S. W. *Nature (London)* **2000**, *406*, 608–611. (b) Badjić, J. D.; Balzani, V.; Credi, A.; Lowe, J. N.; Silvi, S.; Stoddart, J. F. *Chem.–Eur. J.* **2004**, *10*, 1926–1935. (c) Sowa, Y.; Rowe, A. D.; Leake, M. C.; Yakushiji, T.; Homma, M.; Ishijima, A.; Berry, R. M. *Nature (London)* **2005**, *437*, 916–919. (d) Wang, W.; Kaifer, A. E. *Angew. Chem., Int. Ed.* **2006**, *45*, 7042–7046. (e) Nijhuis, C. A.; Ravoo, B. J.; Huskens, J.; Reinhoudt, D. N. *Coord. Chem. Rev.* **2007**, *251*, 1761–1780. (f) Lee, J. W.; Hwang, I.; Jeon, W. S.; Ko, Y. H.; Sakamoto, S.; Yamaguchi, K.; Kim, K. *Chem. Asian J.* **2008**, *3*, 1277–1283.
- (11) (a) Jeon, W. S.; Ziganshina, A. Y.; Lee, J. W.; Ko, Y. H.; Kang, J. K.; Lee, C.; Kim, K. *Angew. Chem., Int. Ed.* **2003**, *42*, 4097–4100. (b) Mobian, P.; Kern, J. M.; Sauvage, J.-P. *Angew. Chem., Int. Ed.* **2004**, *43*, 2392–2395. (c) Norikane, Y.; Tamaoki, N. *Org. Lett.* **2004**, *6*, 2595–2598. (d) Berna, J.; Leigh, D. A.; Lubomska, M.; Mendoza, S. M.; Perez, E. M.; Rudolf, P.; Teobaldi, G.; Zerbetto, F. *Nat. Mater.* **2005**, *4*, 704–710. (e) Raymo, F. M. *Angew. Chem., Int. Ed.* **2006**, *45*, 5249–5251. (f) Credi, A. *Aust. J. Chem.* **2006**, *59*, 157–169. (g) Champin, B.; Mobian, P.; Sauvage, J.-P. *Chem. Soc. Rev.* **2007**, *36*, 358–366. (h) Bonnet, S.; Collin, J. P. *Chem. Soc. Rev.* **2008**, *37*, 1207–1217. (i) Hirose, K.; Shiba, Y.; Ishibashi, K.; Doi, Y.; Tobe, Y. *Chem.–Eur. J.* **2008**, *14*, 3427–3433.
- (12) (a) Balzani, V.; Credi, A.; Venturi, M. *Chem.–Eur. J.* **2002**, *8*, 5524–5532. (b) Murugavel, R.; Walawalkar, M. G.; Dan, M.; Roesky, H. W.; Rao, C. N. R. *Acc. Chem. Res.* **2004**, *37*, 763–774.
- (13) (a) Jager, E. W. H.; Smela, E.; Inganas, O. *Science* **2000**, *290*, 1540–1545. (b) Lin, K. J.; Fu, S. J.; Cheng, C. Y.; Chen, W. H.; Kao, H. M. *Angew. Chem., Int. Ed.* **2004**, *43*, 4186–4189. (c) Ha, S. M.; Yuan, W.; Pei, Q. B.; Pelrine, R.; Stanford, S. *Adv. Mater.* **2006**, *18*, 887–891. (d) Kim, H. J.; Lee, E.; Park, H. S.; Lee, M. J. *Am. Chem. Soc.* **2007**, *129*, 10994–10995. (e) Kushner, A. M.; Gabuchian, V.; Johnson, E. G.; Guan, Z. B. *J. Am. Chem. Soc.* **2007**, *129*, 14110–14111. (f) Mirfakhrai, T.; Madden, J. D. W.; Baughman, R. H. *Mater. Today* **2007**, *10*, 30–38. (g) Murphy, W. L.; Dillmore, W. S.; Modica, J.; Mrksich, M. *Angew. Chem., Int. Ed.* **2007**, *46*, 3066–3069. (h) Feinberg, A. W.; Feigel, A.; Shevokoplyas, S. S.; Sheehy, S.; Whitesides, G. M.; Parker, K. K. *Science* **2007**, *317*, 1366–1370.
- (14) (a) Zhu, S. S.; Swager, T. M. *J. Am. Chem. Soc.* **1997**, *119*, 12568–12577. (b) Clarkson, G. J.; Leigh, D. A.; Smith, R. A. *Curr. Opin. Solid State Mater. Sci.* **1998**, *3*, 579–584. (c) Fyfe, M. C. T.; Stoddart, J. F. *Coord. Chem. Rev.* **1999**, *183*, 139–155. (d) Kim, K. *Chem. Soc. Rev.* **2002**, *31*, 96–107. (e) Cacialli, F.; Wilson, J. S.; Michels, J. J.; Daniel, C.; Silva, C.; Friend, R. H.; Severin, N.; Samori, P.; Rabe, J. P.; O’Connell, M. J.; Taylor, P. N.; Anderson, H. L. *Nat. Mater.* **2002**, *1*, 160–164. (f) Huang, F. H.; Gibson, H. W. *Prog. Polym. Sci.* **2005**, *30*, 982–1018. (g) Wenz, G.; Han, B. H.; Muller, A. *Chem. Rev.* **2006**, *106*, 782–817. (h) Frampton, M. J.; Anderson, H. L. *Angew. Chem., Int. Ed.* **2007**, *46*, 1028–1064. (i) Zhang, W. Y.; Dichtel, W. R.; Stieg, A. Z.; Benítez, D.; Gimzewski, J. K.; Heath, J. R.; Stoddart, J. F. *Proc. Natl. Acad. Sci. U.S.A.* **2008**, *105*, 6514–6519.
- (15) (a) Lukin, O.; Kubota, T.; Okamoto, Y.; Kaufmann, A.; Vögtle, F. *Chem.–Eur. J.* **2004**, *10*, 2804–2810. (b) Tsuda, S.; Aso, Y.; Kaneda, T. *Chem. Commun.* **2006**, 3072–3074. (c) Fuller, A. M. L.; Leigh, D. A.; Lusby, P. J. *Angew. Chem., Int. Ed.* **2007**, *46*, 5015–5019. (d) Wu, J.; Leung, K. C.-F.; Stoddart, J. F. *Proc. Natl. Acad. Sci. U.S.A.* **2007**, *104*, 17266–17271.
- (16) (a) Elizarov, A. M.; Chiu, S. H.; Glink, P. T.; Stoddart, J. F. *Org. Lett.* **2002**, *4*, 679–682. (b) Leung, K. C.-F.; Mendes, P. M.; Magonov, S. N.; Northrop, B. H.; Kim, S.; Patel, K.; Flood, A. H.; Tseng, H.-R.; Stoddart, J. F. *J. Am. Chem. Soc.* **2006**, *128*, 10707–10715. (c) Kim, S. Y.; Ko, Y. H.; Lee, J. W.; Sakamoto, S.; Yamaguchi, K.; Kim, K. *Chem. Asian J.* **2007**, *2*, 747–754.
- (17) Olson, M. A.; Braunschweig, A. B.; Fang, L.; Ikeda, T.; Klajn, R.; Trabolsi, A.; Wesson, P. J.; Benítez, D.; Mirkin, C. A.; Grzybowski, B. A.; Stoddart, J. F. *Angew. Chem., Int. Ed.* **2009**, *48*, 1792–1797.
- (18) (a) Ashton, P. R.; Ballardini, R.; Balzani, V.; Baxter, I.; Credi, A.; Fyfe, M. C. T.; Gandolfi, M. T.; Gómez-López, M.; Martínez-Díaz, M. V.; Piersanti, A.; Spencer, N.; Stoddart, J. F.; Venturi, M.; White, A. J. P.; Williams, D. J. *J. Am. Chem. Soc.* **1998**, *120*, 11932–11942. (b) Badjić, J. D.; Balzani, V.; Credi, A.; Silvi, S.; Stoddart, J. F. *Science* **2004**, *303*, 1845–1849. (c) Garau-dee, S.; Silvi, S.; Venturi, M.; Credi, A.; Flood, A. H.; Stoddart, J. F. *ChemPhysChem* **2005**, *6*, 2145–2152. (d) Braunschweig, A. B.; Ronconi, C. M.; Han, J.-Y.; Aricó, F.; Cantrill, S. J.; Stoddart, J. F.; Khan, S. I.; White, A. J. P.; Williams, D. J. *Eur. J. Org. Chem.* **2006**, 1857–1866.
- (19) (a) Ashton, P. R.; Fyfe, M. C. T.; Hickingbottom, S. K.; Menzer, S.; Stoddart, J. F.; White, A. J. P.; Williams, D. J. *Chem.–Eur. J.* **1998**, *4*, 577–589. (b) Ashton, P. R.; Baxter, I.; Cantrill, S. J.; Fyfe, M. C. T.; Glink, P. T.; Stoddart, J. F.; White, A. J. P.; Williams, D. J. *Angew. Chem., Int. Ed.* **1998**, *37*, 1294–1297. (c) Cantrill, S. J.; Youn, G. J.; Stoddart, J. F.; Williams, D. J. *J. Org. Chem.* **2001**, *66*, 6857–6872. (d) Amirsakis, D. G.; Elizarov, A. M.; Garcia-Garibay, M. A.; Glink, P. T.; Stoddart, J. F.; White, A. J. P.; Williams, D. J. *Angew. Chem., Int. Ed.* **2003**, *42*, 1126–1132. (e) Coutrot, F.; Romuald, C.; Busseron, E. *Org. Lett.* **2008**, *10*, 3741–3744.

–CH<sub>2</sub>NHCH<sub>2</sub>– function. Apparently, reprotonation of the neutral amino group back to a dialkylammonium center results in the return of the DB24C8 ring to this (–CH<sub>2</sub>NH<sub>2</sub><sup>+</sup>CH<sub>2</sub>–) center. Such acid–base switching has proven<sup>18</sup> to be fast and reversible. Engineering the acid–base switchable<sup>2</sup> rotaxane into a [c2]daisy chain topology<sup>19</sup> allows muscle-like contractions and expansions to occur as a result of the acid–base switching of the molecules. Moreover, the facile synthesis and symmetric nature of [c2]daisy chains allow further functionalization and elaboration of the molecule, especially into oligomeric or polymeric scaffolds, without confronting major synthetic challenges. Recently, a polymeric [c2]daisy chain was reported<sup>20</sup> and an acid–base switchable [c2]daisy chain was described.<sup>21</sup>

Herein, we report on (i) the preparation of a series of [c2]daisy chain compounds functionalized with various different end groups, (ii) the synthesis and characterization of a mechanically interlocked poly[c2]daisy chain, and (iii) the investigation of the acid–base switching behavior of both the monomers and the polymer.

## Results and Discussions

**Design and Synthetic Strategy.** A [c2]daisy chain topology has been identified<sup>19–22</sup> wherein (Figure 1) two mechanically interlocked filaments glide along one another through terminal rings and in which the other end of each filament is attached to bulky stoppers to prevent dethreading of the rings. The C<sub>2</sub> axis and inversion center (C<sub>i</sub>), along with the plane of symmetry (σ) present in this structure, make it highly symmetric. Thus, a synthetic approach which allows for the simultaneous elaboration of both filaments was adopted. In this case, to generate the stable [c2]daisy chain structure, a dimeric self-complex of the filament is attached with two end groups that contain bulky stoppers, e.g., 2,6-diisopropyl- and 2,6-di-*tert*-butyl-phenyl groups.

To achieve molecular bistability, both recognition sites for DB24C8, namely, –CH<sub>2</sub>NH<sub>2</sub><sup>+</sup>CH<sub>2</sub>– and BPYM<sup>2+</sup>, must be incorporated into the filament. By taking advantage of the strong binding affinity between DB24C8 and –CH<sub>2</sub>NH<sub>2</sub><sup>+</sup>CH<sub>2</sub>–, which is primarily on account of the convergent [N<sup>+</sup>–H⋯O] interaction, we are able to design a dimeric self-complex precursor in which the DB24C8 and –CH<sub>2</sub>NH<sub>2</sub><sup>+</sup>CH<sub>2</sub>– are covalently linked together. The –CH<sub>2</sub>NH<sub>2</sub><sup>+</sup>CH<sub>2</sub>– site on each filament can thread inside the DB24C8 ring on the other filament in aprotic solvents.

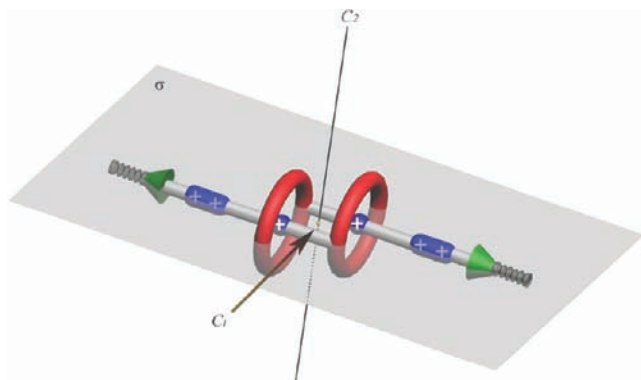


**Figure 1.** A graphic representation of a doubly switchable [c2]daisy chain with C<sub>2</sub>i symmetry. The red rings will have the dibenzo[24]crown-8 constitution. The green stoppers are substituted diisopropylphenyl groups. The recognition sites on the rods attached to the red rings are the more preferred CH<sub>2</sub>NH<sub>2</sub><sup>+</sup>CH<sub>2</sub> recognitions sites (blue spheres) and the less preferred bipyridinium (BYPM<sup>2+</sup>) recognition sites (elongated solid blue cylinders).

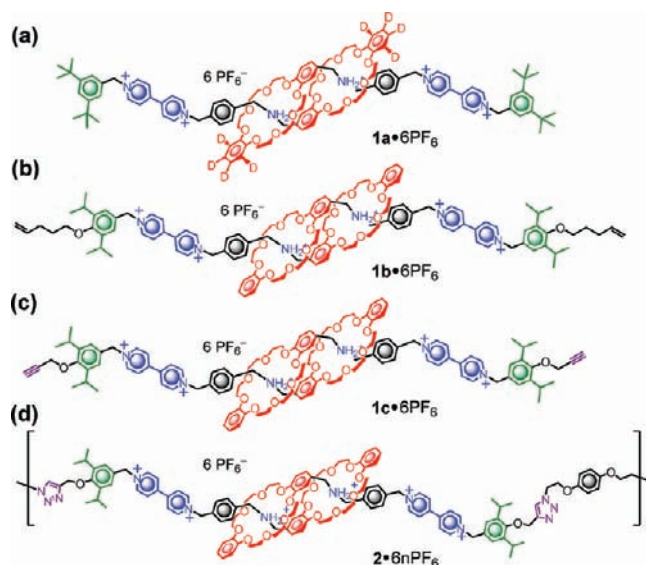


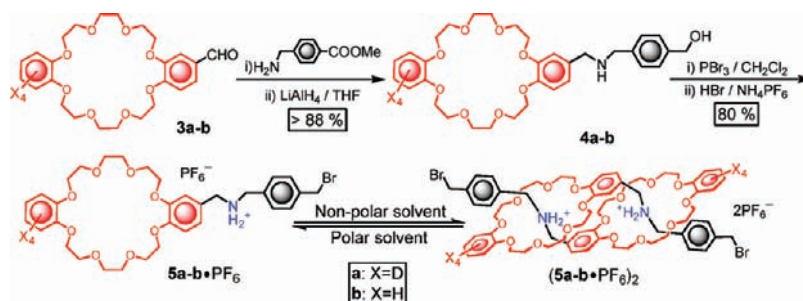
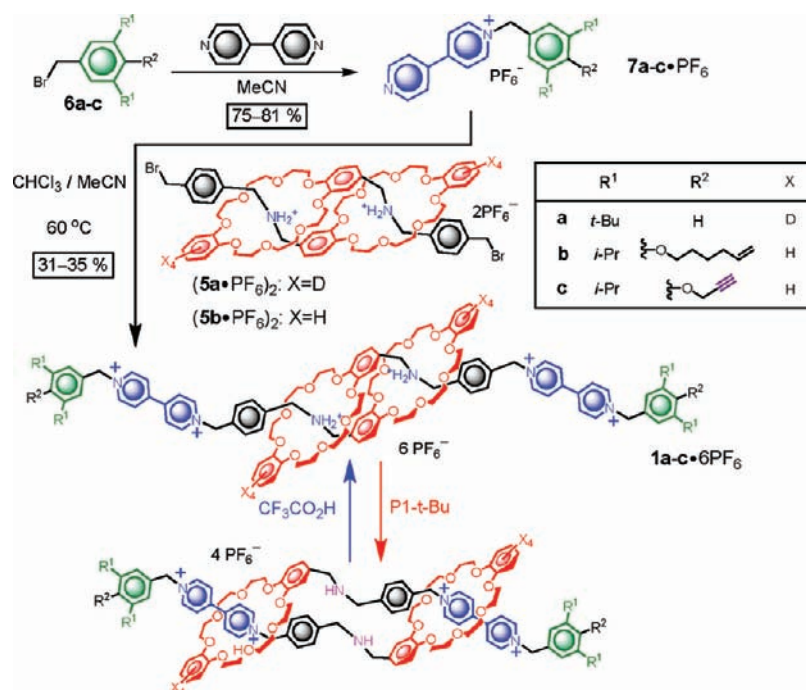
**Figure 2.** Molecular formulas of (a) the model [c2]daisy chain compound **1a**•6PF<sub>6</sub>, (b and c) the functionalized [c2]daisy chain compounds **1b**•6PF<sub>6</sub> and **1c**•6PF<sub>6</sub>, respectively, and finally (d) the poly[c2]daisy chain **2**•6nPF<sub>6</sub>.

An S<sub>N</sub>2 alkylation of the brominated self-complex at both ends with bulky groups which contain the 4-pyridylpyridinium moiety completes the construction of the stoppered [c2]daisy chain molecules, while also generating the second BYPM<sup>2+</sup> recognition site simultaneously. To simplify the NMR spectral interpretation of the resulting products, a DB24C8 ring containing a tetradeuterated catechol ring was incorporated into the model compound.

By functionalizing the stoppers, one can synthesize bistable [c2]daisy chain molecules with various terminal functional groups. Such an AA-type bifunctional compound can undergo polymerization with a compatible BB-type bifunctional compound to afford linear [c2]daisy chain polymers. The highly efficient Cu-catalyzed, Huisgen 1,3-dipolar cycloaddition<sup>14i,23</sup> was chosen for the polymerization step on account of its mild nature and high conversion. The simple reaction conditions required for the polymerization, namely CuI addition with low heating, were mild enough to ensure that the [c2]daisy chain monomer units would not decompose or undergo side reactions. High conversions (typically >99%) are pivotal to stepwise growth polymerizations since the degree of polymerization is heavily dependent on the efficiency of the reaction.

- (20) Guidry, E. N.; Li, J.; Stoddart, J. F.; Grubbs, R. H. *J. Am. Chem. Soc.* **2007**, *129*, 8944–8945.
- (21) Wu, J.-S.; Leung, K. C.-F.; Benítez, D.; Han, J. Y.; Cantrill, S. J.; Fang, L.; Stoddart, J. F. *Angew. Chem., Int. Ed.* **2008**, *47*, 7470–7474.
- (22) (a) Hoshino, T.; Miyauchi, M.; Kawaguchi, Y.; Yamaguchi, H.; Harada, A. *J. Am. Chem. Soc.* **2000**, *122*, 9876–9877. (b) Jimenez, M.-C.; Dietrich-Buchecker, C.; Sauvage, J.-P. *Angew. Chem., Int. Ed.* **2000**, *39*, 3284–3285. (c) Jimenez, M.-C.; Dietrich-Buchecker, C.; Sauvage, J.-P.; De Cian, A. *Angew. Chem., Int. Ed.* **2000**, *39*, 1295–1296. (d) Jimenez-Molero, M.-C.; Dietrich-Buchecker, C.; Sauvage, J.-P. *Chem.—Eur. J.* **2002**, *8*, 1456–1466. (e) Tsukagoshi, S.; Miyawaki, A.; Takashima, Y.; Yamaguchi, H.; Harada, A. *Org. Lett.* **2007**, *9*, 1053–1055. (f) Dawson, R. E.; Lincoln, S. F.; Easton, C. J. *Chem. Commun.* **2008**, 3980–3982. (g) Dawson, R. E.; Maniam, S.; Lincoln, S. F.; Easton, C. J. *Org. Biomol. Chem.* **2008**, *6*, 1814–1821.
- (23) (a) Kolb, H. C.; Finn, M. G.; Sharpless, K. B. *Angew. Chem., Int. Ed.* **2001**, *40*, 2004–2021. (b) van Steenis, D. J. V. C.; David, O. R. P.; van Strijdonck, G. P. F.; van Maarseveen, J. H.; Reek, J. N. H. *Chem. Commun.* **2005**, 4333–4335. (c) Dichtel, W. R.; Miljanić, O. S.; Spruell, J. M.; Heath, J. R.; Stoddart, J. F. *J. Am. Chem. Soc.* **2006**, *128*, 10388–10390.



**Scheme 1.** Synthesis of **5a•PF<sub>6</sub>** and **5b•PF<sub>6</sub>** Which Self-Assemble Spontaneously To Give Dimeric Complexes**Scheme 2.** Synthesis of the Monomeric [c2]Daisy Chain Compounds **1a–c•6PF<sub>6</sub>**

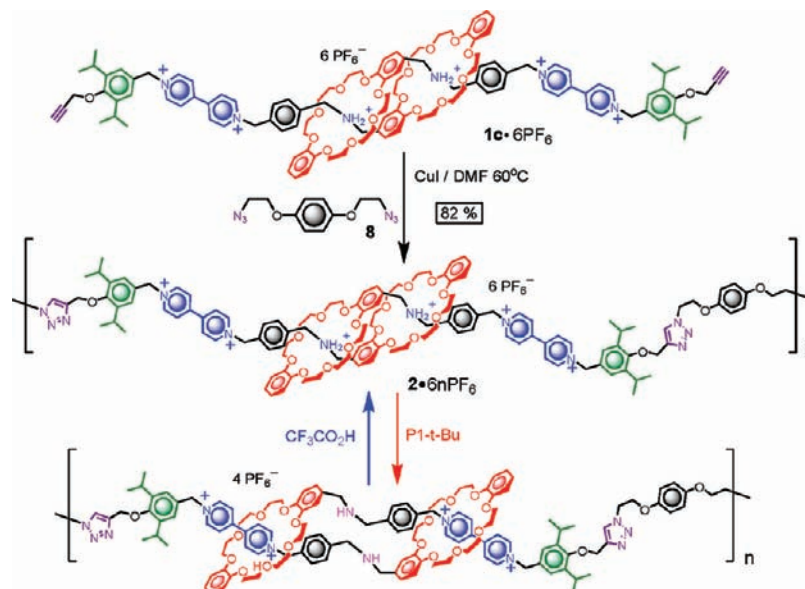
Based on the strategy which has been outlined, a series of monomeric and polymeric daisy chain derivatives (Figure 2) have been identified. The [c2]daisy chain **1a•6PF<sub>6</sub>** (Figure 2a) is a model compound bearing a tetra-deuterated catechol moiety on the DB24C8 rings. The derivatives **1b•6PF<sub>6</sub>** (Figure 2b) and **1c•6PF<sub>6</sub>** (Figure 2c) are terminally functionalized on their stoppers by 1-pentyl and propargyl groups, respectively. **2•6nPF<sub>6</sub>** (Figure 2d) represents the linear polymeric [c2]daisy chain derived from **1c•6PF<sub>6</sub>**. With these compounds in hand, a muscle-like contraction–extension can be triggered by addition of bases and acids. In this report, the non-nucleophilic bases, 1,4-diaza-bicyclo[2,2,2]octane (DABCO) and *N*-*tert*-butyl-hexamethylphosphortriamide (phosphazene base referred to as P1-*t*-Bu), were chosen to initiate the base-triggered molecular contraction by fully deprotonating the  $-\text{CH}_2\text{NH}_2^+\text{CH}_2-$  centers, while leaving the BYPM<sup>2+</sup> units intact. On the other hand, trifluoroacetic acid was used for reprotonation of  $-\text{CH}_2\text{NH}-\text{CH}_2-$  functions to promote the reverse extension movement.

**Synthesis.** The synthetic routes employed for the fabrication of both the tetra-deuterated and nondeuterated dimeric superstructures (**5a–b•PF<sub>6</sub>**)<sub>2</sub>, the [c2]daisy chains **1a–c•6PF<sub>6</sub>**, and the polymeric [c2]daisy chain **2•6nPF<sub>6</sub>** are outlined in Schemes 1–3. The preparation of (**5a–b•PF<sub>6</sub>**)<sub>2</sub> began with reductive amination of the formylated DB24C8 derivatives **3a–b** with methyl 4-(aminomethyl)benzoate. Lithium aluminum hydride

reduced the imine bonds and the ester groups to secondary amine and benzylic alcohol functions, respectively, in one pot. Bromination of the benzylic alcohol using phosphorus tribromide, followed by protonation of the amine using hydrobromic acid and counterion exchange using NH<sub>4</sub>PF<sub>6</sub>, gave **5a–b•PF<sub>6</sub>**, which forms a dimeric self-complex (**5a–b•PF<sub>6</sub>**)<sub>2</sub> in an aprotic solvent such as MeCN. Formation of (**5a–b•PF<sub>6</sub>**)<sub>2</sub> was confirmed (see Supporting Information) by the  $[2M - 2\text{PF}_6]^{2+}$  peak found in an electrospray ionization mass spectrum (ESI-MS) of **5b•PF<sub>6</sub>** using MeCN as the solvent.<sup>24</sup>

To complete the construction (Scheme 2) of [c2]daisy chain molecules, the 4-pyridylpyridinium-containing bulky stoppers **7a–c•PF<sub>6</sub>** were prepared by reacting 4,4'-bipyridine with the benzyl bromide derivatives **6a–c**. A mixed solvent system (CHCl<sub>3</sub>/MeCN, *v/v* = 1:1) was chosen to optimize the reaction yield by balancing both the solubility and polarity. By treating **7a•PF<sub>6</sub>** with (**5a•PF<sub>6</sub>**)<sub>2</sub> in this solvent mixture at 55 °C, the doubly threaded [c2]daisy chain model compound **1a•6PF<sub>6</sub>** was formed and isolated in >30% yield. Using the same method,

(24) A single positively charged peak at  $m/z = 660.622 [M - \text{PF}_6]^+$  was revealed when MeOH was used as the solvent for electrospray ionization; on the contrary, a doubly positive charged peak at  $m/z = 660.640 [2M - 2\text{PF}_6]^{2+}$  was observed when using MeCN, indicating the formation of dimeric species (see Supporting Information).

Scheme 3. Synthesis of the Poly[*c*2]daisy Chain **2**•6nPF<sub>6</sub> and the Acid–Base Switching Process

**1b**–**c**•6PF<sub>6</sub> were synthesized successfully by reacting **7b**–**c**•PF<sub>6</sub> with (**5b**•PF<sub>6</sub>)<sub>2</sub>.

The synthesis of the linear main-chain poly[*c*2]daisy chain **2**•6nPF<sub>6</sub> is outlined in Scheme 3. As a terminally bifunctionalized compound, **1c**•6PF<sub>6</sub> was subjected to a step-growth AA+BB type polymerization using the Cu-catalyzed Huisgen 1,3-dipolar cycloaddition<sup>14i</sup> with 1 equiv of the diazide **8** in the presence of a stoichiometric amount of CuI in DMF-*d*<sub>7</sub>, to afford the linear main chain poly[*c*2]daisy chain **2**•6nPF<sub>6</sub>. <sup>1</sup>H NMR spectroscopy was employed to monitor the reaction process by tracking the disappearance of the alkyne signal and the appearance of the newly formed triazole proton resonance.

**Structural Characterization.** The <sup>1</sup>H NMR spectrum of **1a**•6PF<sub>6</sub> in CD<sub>3</sub>CN reveals well-resolved peaks, which were assigned with the help of COSY-NMR 2D correlations. The spectra indicate that the DB24C8 rings exhibit an overwhelming selectivity to encircle the –CH<sub>2</sub>NH<sub>2</sub><sup>+</sup>CH<sub>2</sub>– recognition sites at room temperature. Two sets of signals for the catechol rings were identified in the region 6.1–7.0 ppm, indicating the

presence of two diastereoisomers. On account of the unsymmetrical substitution of the DB24C8 ring, dimerization gives (Figure 3) two C<sub>2</sub>-symmetrical (chiral) enantiomers and a C<sub>i</sub>-symmetrical (meso) diastereoisomer.

Compounds **1b**–**c**•6PF<sub>6</sub> exhibit <sup>1</sup>H NMR resonances similar to **1a**•6PF<sub>6</sub>, except for the addition of signals arising from the catechol protons and the terminal alkene and alkyne residues (see Supporting Information). High resolution ESI mass spectra of **1a**–**c**•6PF<sub>6</sub> all afforded multiply charged peaks, i.e., [M – 2PF<sub>6</sub>]<sup>2+</sup>, as a result of the loss of multiple PF<sub>6</sub><sup>–</sup> counterions during the ionization processes.

The <sup>1</sup>H NMR spectrum of the polymer **2**•6nPF<sub>6</sub> in CD<sub>3</sub>CN shows well-resolved signals reminiscent of those present in the monomeric precursor **1c**•6PF<sub>6</sub>. With each repeating unit connected to one another by mechanical bonds, **2**•6nPF<sub>6</sub> is a “true” macromolecule and is expected to have properties characteristic of a polymer. Chronocoulometry measurement (Figure 4a) carried out on **2**•6nPF<sub>6</sub> gave a diffusion coefficient of (2.52 ± 0.06) × 10<sup>–10</sup> m<sup>2</sup>/s, a value which is much smaller than that [(7.95 ± 0.10) × 10<sup>–10</sup> m<sup>2</sup>/s] of the monomer **1c**•6PF<sub>6</sub>, suggesting that **2**•6nPF<sub>6</sub> has a much longer hydrodynamic radius than the monomer. Size exclusion chromatography/multiangle light scattering (SEC-MALS) analysis of **2**•6nPF<sub>6</sub>, which was performed using a solution of NH<sub>4</sub>PF<sub>6</sub> in DMF (0.2 mol/L) as the eluent,<sup>25</sup> showed (Figure 4b) a major peak in the chromatograph, with a small amount of unreacted monomer. The calculated number average molecular weight (*M*<sub>n</sub>) is 32.9 ± 2.5 kDa with a polydispersity index (PDI) of 1.85 from Zimm plot analysis. The *M*<sub>n</sub> indicates that, on average, each polymer chain is composed of ~11 repeating units. As a control experiment, SEC-MALS analysis of the monomer **1c**•6PF<sub>6</sub> resulted in a sharp peak with molecular weight of 4 kDa, a value which is of the same order of magnitude (2.8 kDa) as the actual molecular weight.<sup>26</sup> Moreover, differential scanning calorimetry (DSC) analysis of **2**•6nPF<sub>6</sub> showed (see Supporting Information)

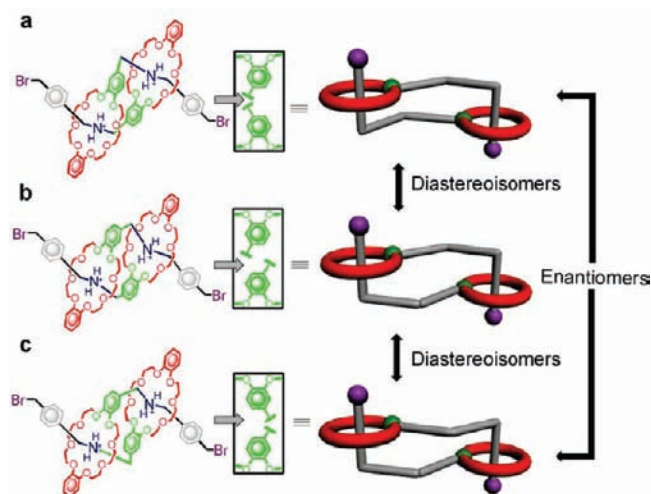


**Figure 3.** Molecular formulas and graphical representation of isomeric superstructures of (**5b**•PF<sub>6</sub>)<sub>2</sub>: (a) and (c) a pair of enantiomers, (b) a meso molecule with a C<sub>i</sub> symmetry; (b) and (a/c) diastereoisomers.

(25) SEC-MALS analysis of **2**•6nPF<sub>6</sub> using pure DMF as the eluent gave a molecular weight of 1466 kDa. Such a large molecular weight can be ascribed to aggregation in a non-electrolyte solution. It is well known that the aggregation of polyelectrolytes can be prevented by introducing ions in concentration into solutions.

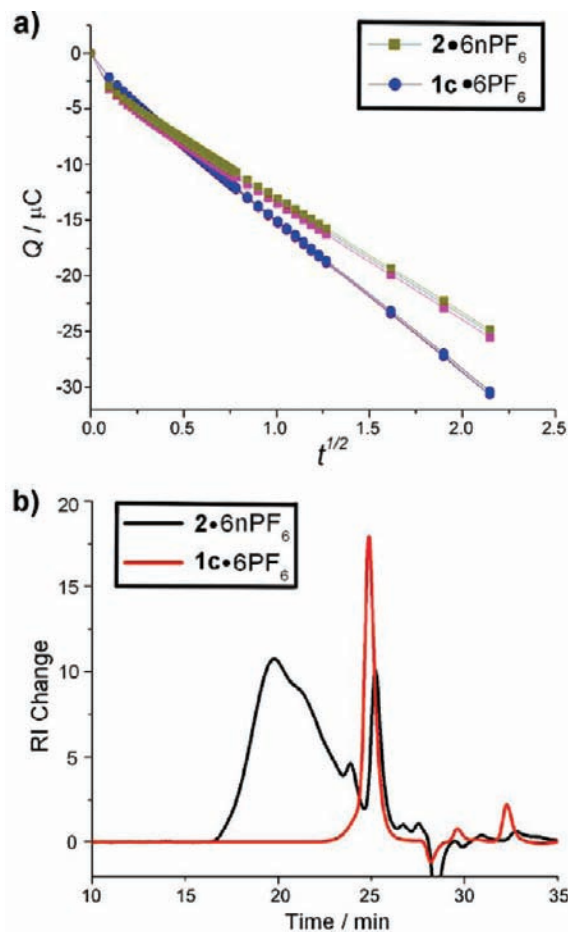


**Figure 4.** Size characterization data for **2•6nPF<sub>6</sub>** and **1c•6PF<sub>6</sub>**: (a) The chronocoulometric response of **2•6nPF<sub>6</sub>** and **1c•6PF<sub>6</sub>** in MeCN. Three parallel experimental plots for the Coulomb value versus the square root of the time are shown for each sample. (b) SEC chromatogram of **2•6nPF<sub>6</sub>** (black) and **1c•6PF<sub>6</sub>** (red) eluted by 0.2 mol/L  $\text{NH}_4\text{PF}_6$  in DMF through two ViscoGEL columns. The concentration detector was the refractive index.

a characteristic, reversible glass transition process at 138 °C, while no melting/crystallization process can be observed up to 250 °C. To conclude, the linear mechanically bonded polymer **2•6nPF<sub>6</sub>** is a large macromolecule as evidenced by (i) its diffusion coefficient, (ii) SEC behavior, (iii) light-scattering properties, and (iv) DSC analysis.

**Acid–Base Switching Monitored by <sup>1</sup>H NMR Spectroscopy.** The acid/base stimulated contractions/extensions of **1a•6PF<sub>6</sub>** and **2•6nPF<sub>6</sub>** were investigated (Figure 5) by <sup>1</sup>H NMR spectroscopy. On adding 2.1 equiv of phosphazene base  $\text{P}_1$ -*t*-Bu, basified **1a•6PF<sub>6</sub>** shows (Figure 5a–b) dramatic signal shifts compared to those for the original protonated material, which revealed that the DB24C8 rings had migrated to the BYPM<sup>2+</sup> recognition sites on deprotonation of the  $-\text{CH}_2\text{NH}_2^+\text{CH}_2-$  centers. Following reprotonation of the  $-\text{CH}_2\text{NHCH}_2-$  unit by 2 equiv of  $\text{CF}_3\text{CO}_2\text{D}$ , the <sup>1</sup>H NMR spectrum is restored (Figure 5c) completely.

The evidence for the DB24C8 ring shuttling after adding base in **1a•6PF<sub>6</sub>** is provided by the fact that (1) the peaks for the

protons ( $H_d$  and  $H_e$ ) on the phenylene spacers are shifted to higher field because of the mutually  $\pi$  overlapping nature of the paraphenylene ring systems in the contracted geometry, (2) the separate peaks for  $H_a$ ,  $H_b$ , and  $H_c$  in the diastereoisomers are less anisochronous and give only one set of accidentally equivalent signals because of the lack of  $\pi$ – $\pi$  interactions of the monosubstituted catechol ring, and (3)  $H_7$  is shifted to higher field while  $H_6$  retains its original chemical shift, thus the encircling position of DB24C8 rings can be assigned primarily to that half-end of BYPM<sup>2+</sup> unit which is close to  $H_7$ . It is also interesting that the signal for the two protons of  $H_7$  changed from an accidentally equivalent singlet to an AB-type system as a result of the increased anisochronous environment after the crown ether ring shuttles onto the BYPM<sup>2+</sup> unit. This assignment is supported by the signal separation of the BYPM<sup>2+</sup> proton ( $\alpha$ 's and  $\beta$ 's) as a result of amplification of the unsymmetrical BYPM<sup>2+</sup> units when the DB24C8 rings encircle only half of them. Although more complicated spectra were recorded when conducting the acid–base switching cycle on **2•6nPF<sub>6</sub>**, the observed <sup>1</sup>H NMR signal movements, reminiscent (Figure 5d–f) of those of **1a•6PF<sub>6</sub>**, can be fully rationalized. This <sup>1</sup>H NMR response demonstrates that the switchability of the polymer **2•6nPF<sub>6</sub>** under acid/base control is of the same magnitude as that of the monomer **1a•6PF<sub>6</sub>**.

**Acid–Base Switching Monitored by UV/vis Absorption Spectroscopy.** UV/vis absorption spectroscopic investigations of both the polymer **2•6nPF<sub>6</sub>** (Figure 6) and the monomer **1c•6PF<sub>6</sub>** (see Supporting Information) in MeCN show similar reversible acid–base switching behavior. Upon the addition (Figure 6a) of DABCO, the absorption band of **2•6nPF<sub>6</sub>**, centered at 260 nm, which originates from the BYPM<sup>2+</sup> units, experiences a significant hypochromic shift, while a new absorption band appears at 390 nm as a result of the charge-transfer interactions between the  $\pi$ -electron deficient BYPM<sup>2+</sup> units and the  $\pi$ -electron rich DB24C8 rings. Upon adding (Figure 6b)  $\text{CF}_3\text{CO}_2\text{H}$  to the basified solution, the same spectroscopic signatures undergo a reversal to lead to the initial state. Isosbestic points at 239, 328, and 343 nm in both titration experiments show unambiguously the contribution of only two species during these titrations. The acid–base titrations demonstrate (Figure 6c) that quantitative and reversible switching processes occur over 2 equiv of either acid or base. Switching cycles of the polymer were also investigated by absorption spectrophotometry at 390 nm (Figure 6d). The “on–off” behavior of **2•6nPF<sub>6</sub>**, triggered by acid/base, remains clearly evident after 10 cycles.

**Acid–Base Switching of the Polymer Monitored by Cyclic Voltammetry.** It is well documented<sup>18</sup> that the switching of similar types of bistable systems can be monitored by cyclic voltammetry (CV) measurements which address the redox active BYPM<sup>2+</sup> units. The bistability of polymer **2•6nPF<sub>6</sub>** was also investigated using this method. The CV scans of **2•6nPF<sub>6</sub>** display (Figure 7) two reduction peaks of the BYPM<sup>2+</sup> units at  $-370$  and  $-797$  mV (vs  $\text{Ag}/\text{AgCl}$ ), respectively. On addition of 2 equiv of  $\text{P}_1$ -*t*-Bu, deprotonation shifts the first reduction process of the BYPM<sup>2+</sup> units strongly toward more negative potentials ( $-477$  mV). Observation of this displacement, together with the <sup>1</sup>H NMR and UV/vis spectroscopic results, indicate<sup>27</sup> that

(26) This disparity in molecular weight from SEC-MALS is primarily on account of the small size of the monomer since low molecular weight species result in weaker scattered laser light and a low signal/noise ratio. Moreover, because the shape of the monomer is neither a random coil nor a perfect rigid rod, the Zimm plot analysis for static light scattering cannot fit the data perfectly to either of the polymer light-scattering function models.

(27) Stoddart, J. F.; et al. *J. Am. Chem. Soc.* **1992**, *114*, 193–218.

(28) The separation of the second reduction peak after addition of  $\text{CF}_3\text{CO}_2\text{H}$  can be attributed to the presence of different counterions ( $\text{PF}_6^-$  and  $\text{CF}_3\text{CO}_2^-$ ) associated with the BYPM<sup>2+</sup> unit.

(29) For details of the kinetics mechanism, see Supporting Information.



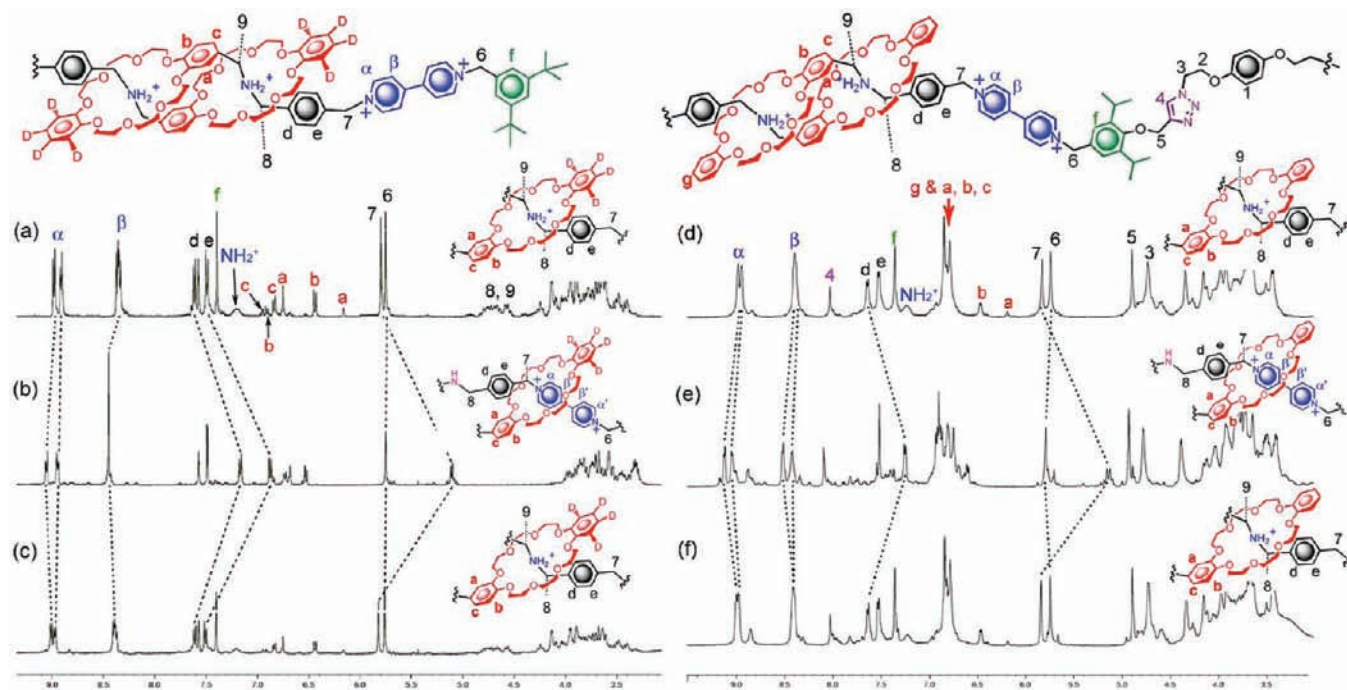


**Figure 5.**  $^1\text{H}$  NMR spectra of  $1\mathbf{a}\cdot 6\text{PF}_6$  (400 MHz) and  $2\cdot 6\text{nPF}_6$  (500 MHz) in  $\text{CD}_3\text{CN}$ : (a) The original spectrum of  $1\mathbf{a}\cdot 6\text{PF}_6$  with peak assignments, (b)  $1\mathbf{a}\cdot 6\text{PF}_6$  after addition of 2 equiv of  $\text{P}_1\text{-}t\text{-Bu}$ , and (c)  $1\mathbf{a}\cdot 6\text{PF}_6$  after further addition of 2.5 equiv of  $\text{CF}_3\text{CO}_2\text{D}$ ; (d) the original spectrum of  $2\cdot 6\text{nPF}_6$  with peak assignments, (e)  $2\cdot 6\text{nPF}_6$  after addition of 2 equiv of  $\text{P}_1\text{-}t\text{-Bu}$ , and (f)  $2\cdot 6\text{nPF}_6$  after further addition of 2.5 equiv of  $\text{CF}_3\text{CO}_2\text{D}$ .

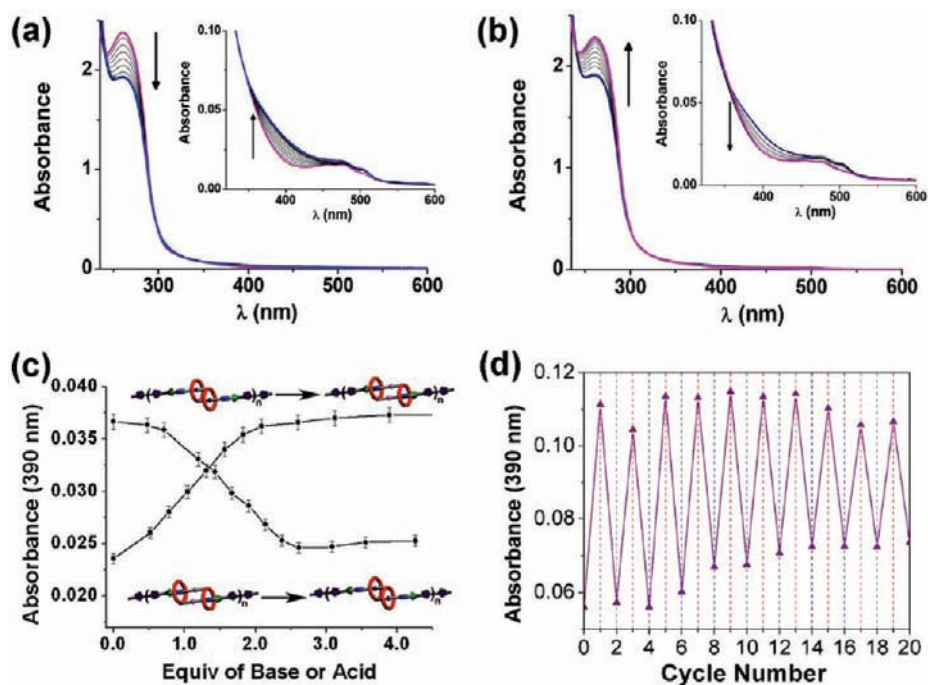


**Figure 6.** UV-vis absorption spectrophotometric variations recorded in MeCN upon (a) addition of DABCO to a solution of  $2\cdot 6\text{nPF}_6$  and (b) further addition of  $\text{CF}_3\text{CO}_2\text{H}$  to a solution of deprotonated  $2\cdot 6\text{nPF}_6$ .  $c_{2\cdot 6\text{nPF}_6} = 4.4 \times 10^{-5}$  mol/L based on the repeating units;  $T = 25.0(2)^\circ\text{C}$ ;  $l = 1$  cm. (c) Variation in the absorbance of the charge transfer band ( $\lambda = 390$  nm) with the gradual addition of DABCO or  $\text{CF}_3\text{CO}_2\text{H}$  to  $2\cdot 6\text{nPF}_6$  in MeCN. (d) The absorbance at 390 nm on conducting 10 acid–base switching cycles (normalized by dilution factor).

the BYPM $^{2+}$  units are engaged in donor–acceptor interactions within the polymer chain, a fact that is consistent with the shuttling of the DB24C8 rings from the  $-\text{CH}_2\text{NH}_2^+\text{CH}_2-$  centers to the BYPM $^{2+}$  sites upon deprotonation of the former. Reprotonation of  $2\cdot 6\text{nPF}_6$  by  $\text{CF}_3\text{CO}_2\text{H}$  leads to the recovery of the first reduction peak $^{28}$  of the BYPM $^{2+}$  unit at  $-350$  mV.

**Dynamics of the [c2]Daisy Chain Systems.** The kinetics of the acid-induced extension and the base-promoted contraction processes of the [c2]daisy chain molecules in MeCN were studied using stopped-flow spectrophotometry techniques. Kinetic measurements were therefore carried out under pseudo-first-order conditions; the acid and base were added in large

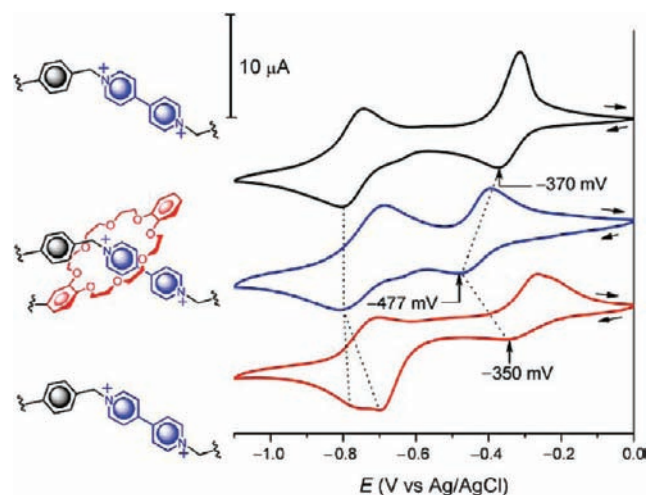


**Figure 7.** Cyclic voltammetry scans (black line) of  $2\bullet 6nPF_6$ , its deprotonated (blue line) and reprotonated (red line) forms ( $c2\bullet 6nPF_6 = 7.5 \times 10^{-4}$  mol/L based on the repeating units) in MeCN, scan rate = 200 mV/s.

excess, e.g., more than 10 equiv. A single-exponential signal versus time (see Figure 8a for  $2\bullet 6nPF_6$ ; see Supporting Information for  $1c\bullet 6PF_6$ ) was recorded while monitoring the CT absorption band at 390 nm.<sup>29</sup>

For the two [c2]daisy chain compounds ( $1c\bullet 6PF_6$  and  $2\bullet 6nPF_6$ ) considered in this work, the pseudo-first-order rate constants ( $k_{obs}$ ) were determined. For the polymer  $2\bullet 6nPF_6$ , the variations of the corresponding  $k_{obs}$  with  $[DABCO]_{tot}$  and with  $[CF_3CO_2H]_{tot}$  are given in Figure 8b–c (for monomer  $1c\bullet 6PF_6$ , see Supporting Information).<sup>29</sup>

We propose the acid/base switching mechanism in Figure 9 for the [c2]daisy chain monomer  $1c^{6+}$  and the polymer  $2^{6n+}$ , respectively.<sup>29</sup> Deprotonations of the  $(-CH_2NH_2^+CH_2-)$  sites in  $1c^{6+}$  and  $2^{6n+}$ , as well as protonations of the  $(-CH_2NHCH_2-)$  centers within  $1c^{4+}$  and  $2^{4n+}$ , are acid–base equilibria which are reached within the mixing time ( $\sim 3$  ms) of the stopped-flow technique.<sup>18c</sup> For the deprotonation of the  $(-CH_2NH_2^+CH_2-)$  units in  $1c^{6+}$  and  $2^{6n+}$  systems, no spectrophotometric variation at 390 nm was observed during the mixing time.

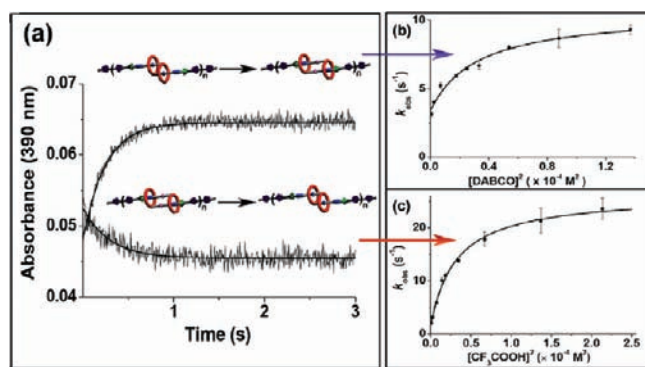


**Figure 8.** (a) Variation of the absorbance at  $\lambda = 390$  nm versus time for the base-induced contraction (top) and the acid-promoted extension (bottom) of the [c2]daisy chain polymer  $2\bullet 6nPF_6$  in MeCN.  $c2\bullet 6nPF_6 = 6.6 \times 10^{-5}$  mol/L based on the repeating units (top)  $c2\bullet 6nPF_6 = 7.05 \times 10^{-5}$  mol/L based on the repeating units (bottom);  $cDABCO = cCF_3CO_2H = 1.56 \times 10^{-3}$  mol/L;  $T = 25.0(2)^\circ C$ . (b) Pseudo-first-order rate constants  $k_{obs}$  ( $s^{-1}$ ) relative to the base-induced contraction of  $2\bullet 6nPF_6$  as a function of  $cDABCO$  ( $c2\bullet 6nPF_6 = 6.6 \times 10^{-5}$  mol/L based on the repeating units) and (c) acid-triggered extension of deprotonated  $2\bullet 6nPF_6$  as a function of  $cCF_3CO_2H$ , ( $c2\bullet 6nPF_6 = 7.05 \times 10^{-5}$  mol/L based on the repeating units), respectively.

Therefore, we suggest that the arrangement of the noncontracted  $1c^{4+*}$  and  $2^{4n+*}$  kinetic intermediates is comparable to that of  $1c^{6+}$  and  $2^{6n+}$ , most likely because of the  $\pi$ – $\pi$  stacking interactions of the substituted catechol rings of the DB24C8 macrocycles.<sup>19c,21</sup> Strikingly, protonation of the  $(-CH_2NH-CH_2-)$  units in  $1c^{4+}$  and  $2^{4n+}$  leads to kinetic intermediates  $1c^{6+*}$  and  $2^{6n+*}$ , whose spectral properties are markedly different from those of the parent  $1c^{4+}$  and  $2^{4n+}$  species. A significant absorption decrease at 390 nm (CT transitions) during the  $\sim 3$  ms dead time suggests that significant electrostatic interactions between the two positively charged  $(-CH_2NH_2^+CH_2-)$  centers in  $1c^{6+*}$  and  $2^{6n+*}$  intermediates destabilize the CT complexes between the dibenzo[24]crown-8 encircling macrocycles and the dialkylated viologen units. As a consequence, the shuttling process was found to be faster in this direction (Figure 8c).

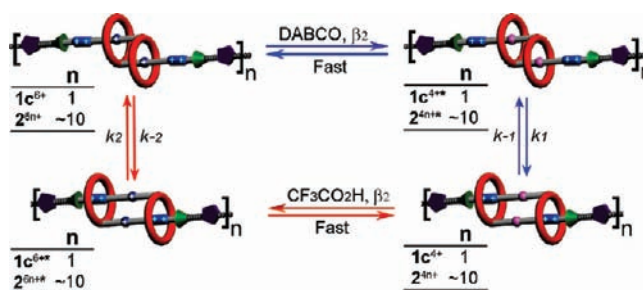


**Figure 9.** Proposed mechanisms for the acid/base switching processes of  $1c\bullet 6PF_6$  and  $2\bullet 6nPF_6$ . Wherein  $\beta_2$  is the deprotonation constant of the dialkylammonium centers or protonation constant of the dialkylamine units,  $k_1$  and  $k_{-1}$  are the forward and backward rate constants for the contraction movement.  $k_2$  and  $k_{-2}$  are the forward and backward rate constants for the extension movement.

The various acid–base reactions are therefore considered as fast pre-equilibria and afford kinetic intermediates with different protonation states. The rate-limiting steps therefore correspond to either the contraction of the kinetic intermediates  $1c^{4+*}$  or  $2^{4n+*}$  or the extension of  $1c^{6+*}$  and  $2^{6n+*}$ . Nonlinear least-squares fittings of the variations of  $k_{obs}$  versus  $[DABCO]_{tot}^2$  and  $[CF_3CO_2H]_{tot}^2$  (Figure 8b–c and Supporting Information) allowed us to determine (Table 1) the monomolecular rate constants  $k_1$ ,  $k_{-1}$ ,  $k_2$ , and  $k_{-2}$  ( $s^{-1}$ ) relative to the contraction and extension processes of  $1c^{6+}$  and of  $2^{6n+}$ , respectively (with  $k_{obs} = (k_1\beta_2[DABCO]_{tot}^2)/(1 + \beta_2[DABCO]_{tot}^2 + k_{-1})$  and  $k_{obs} = (k_2\beta_1[CF_3COOH]_{tot}^2)/(1 + \beta_1[CF_3COOH]_{tot}^2 + k_{-2})$ ).<sup>30</sup>

Both  $1c^{6+}$  and  $2^{6n+}$  exerted faster  $CF_3CO_2H$ -induced extension than DABCO-induced contraction. Indeed,  $k_2$  values [ $15.5(6) s^{-1}$  for  $\sim 1c^{6+*} \rightarrow 1c^{6+}$  and  $24.7(8) s^{-1}$  for  $2^{6n+*} \rightarrow 2^{6n+}$ ] are approximately three times higher than the corresponding  $k_1$  values [ $5.7(6) s^{-1}$  for  $\sim 1c^{4+*} \rightarrow 1c^{4+}$  and  $7.2(5) s^{-1}$  for  $2^{4n+*} \rightarrow 2^{4n+}$ ]. These data agree well with the kinetic parameters previously reported for a related acid–base-switchable [2]rotaxane.<sup>18c</sup> In both cases, backward rate constants  $k_{-1}$  or  $k_{-2}$  were also measured, suggesting possible redistribution processes. The association constants between DB24C8 and dibenzylammonium dication/4,4'-bipyridinium dication are 420 and 82  $M^{-1}$  in MeCN, respectively.<sup>18a,d</sup> The larger  $k_2/k_{-2}$  values ( $\sim 4.0$  for  $1c^{6+}$  and  $\sim 15.4$  for  $2^{6n+}$ ) compared to the  $k_1/k_{-1}$

(30)  $\beta_2$  is the global protonation or deprotonation constant of the [c2]daisy chain molecules,  $k_1$  is the monomolecular rate constant of the base-induced contraction movement within the [c2]daisy chain molecules, while  $k_{-1}$  is the backward monomolecular rate constant of the contraction.  $k_2$  and  $k_{-2}$  describe the same processes for the acid-induced extension processes.



**Table 1.** Kinetic Parameters<sup>a</sup> for the Base-Induced Contraction ( $k_1$  and  $k_{-1}$ ) and Acid-Promoted Extension ( $k_2$  and  $k_{-2}$ ) Processes of the [c2]Daisy Chain Monomer **1c**•6PF<sub>6</sub> and Polymer **2**•6nPF<sub>6</sub>

		$\log \beta_2$	$k_1(3\sigma)/s^{-1}$	$k_2(3\sigma)/s^{-1}$	$k_{-1}(3\sigma)/s^{-1}$	$k_{-2}(3\sigma)/s^{-1}$
base-triggered contraction	<b>1c</b> <sup>6+</sup> → <b>1c</b> <sup>4+</sup>	4.9 ± 0.2	5.7 ± 0.6		3.0 ± 0.5	
	<b>2</b> <sup>6n+</sup> → <b>2</b> <sup>4n+</sup>	4.5 ± 0.3	7.2 ± 0.5		3.4 ± 0.3	
acid-triggered extension	<b>1c</b> <sup>4+</sup> → <b>1c</b> <sup>6+</sup>	4.6 ± 0.2		15.5 ± 0.6		3.8 ± 0.3
	<b>2</b> <sup>4n+</sup> → <b>2</b> <sup>6n+</sup>	4.5 ± 0.1		24.7 ± 0.8		1.60 ± 0.05

<sup>a</sup> Solvent: MeCN,  $T$ : 25.0(2) °C. Errors =  $3\sigma$  with  $\sigma$  = standard deviation.

$k_{-1}$  values ( $\sim 2.0$  for **1c**<sup>4+</sup> and **2**<sup>4n+</sup>) are indicative of a better selectivity of DB24C8 rings for (–CH<sub>2</sub>NH<sub>2</sub><sup>+</sup>CH<sub>2</sub>–) centers over BYPM<sup>2+</sup> units than that on BYPM<sup>2+</sup> units over neutral (–CH<sub>2</sub>NHCH<sub>2</sub>–) units. Interestingly, we also observed that the shuttling processes are faster for the polymeric derivative **2**•6nPF<sub>6</sub> than for the monomer **1c**•6PF<sub>6</sub>. Speeding up of the reactions **2**<sup>4n+\*</sup> → **2**<sup>4n+</sup> or **2**<sup>6n+\*</sup> → **2**<sup>6n+</sup> is indeed measured, a trend which suggests that the shuttling of the other subunits becomes faster after the translocation of the first subunit in the polymer. A similar cooperative kinetics effect, which depends on  $\pi$ -electron donor–acceptor interactions for switching, was observed<sup>17</sup> on a bistable side-chain polycatenane. This polymer-promoted switching rate enhancement is under further investigation.

## Conclusions

The syntheses and characterization of a series of bistable [c2]daisy chain derivatives and a linear polymeric analogue have been reported. The versatile synthetic strategy enables amenable structural modifications of these acid–base switchable, doubly threaded architectures. The polymeric properties, namely, a low diffusion coefficient and a large SEC molecular weight, of the poly[c2]daisy chain demonstrate that the mechanical bonds are equivalent to covalent bonds in terms of their size effects. Extensive investigations of the pH-controlled switching mech-

anism revealed that both the monomer units and the polymeric ensemble display quantitative and fully reversible switching behavior in solution. Faster switching rates for both contraction and extension processes were observed on the polymer compared to its monomeric precursor. This robust polymeric switchable material sets the stage for the development of smart materials and functional nanomachinery.

**Acknowledgment.** This research was supported by the U.S. Air Force Office of Scientific Research (AFOSR: FA9550-08-1-0349) and by the Centre National de la Recherche Scientifique (UDS/CNRS UMR 7177) in France. L.F. gratefully acknowledges the support of a Ryan Fellowship from Northwestern University. M.H. is supported by a Doctoral Fellowship from the French Ministry of Research and Education. J.M.S. gratefully acknowledges the National Science Foundation for a Graduate Research Fellowship.

**Supporting Information Available:** Experimental procedures. Mass spectra and NMR spectra of key compounds. Additional UV/vis absorption spectra and kinetics measurement data. Complete ref 27. These materials are available free of charge via the Internet at <http://pubs.acs.org>.

JA900859D